Am J Transl Res 2018;10(8):2372-2386
www.ajtr.org /ISSN:1943-8141/AJTR0077496

Original Article

Transcriptomic profile analysis of brain microvascular pericytes in spontaneously hypertensive rats by RNA-Seq

Xiaochen Yuan[1,2*], Qingbin Wu[1,2*], Xueting Liu[1,2], Honggang Zhang[1,2], Ruijuan Xiu[1,2]

[1]Key Laboratory for Microcirculation, Ministry of Health, Beijing, China; [2]Institute of Microcirculation, Chinese Academy Medical Sciences & Pecking Union Medical College, Beijing, China. [*]Equal contributors.

Received April 7, 2018; Accepted July 12, 2018; Epub August 15, 2018; Published August 30, 2018

Abstract: Background: Changes in the structure and function of micro-vessels is the pathogenic basis of organ damage in cardiovascular and cerebrovascular diseases. Microcirculation is primarily affected in hypertension, resulting in increased vascular resistance. Pericytes are contractile cells that are embedded in the basement membrane of capillaries, and regulate endothelial cell membrane maturation, capillary blood flow, cell debris removal, and stability of endothelial cells. However, the exact role of brain microvascular pericytes in the pathogenesis of hypertension has not been elucidated. Methods: Brain microvascular pericytes were isolated from spontaneously hypertensive rats (SHR) and wild type Wistar Kyoto (WKY) rats. The transcriptomes of SHR and WKY pericytes were analyzed by RNA-Seq, and the differentially expressed genes (DEGs) were screened by Ballgown, and Student's t test was used to be used to compare differences between groups. DAVID was used for the GO-enrichment analysis and KEGG pathway analysis of the DEGs, and an interaction network between the significant signaling pathways and DEGs was constructed. Results: A total of 1356 DEGs were identified between the WKY and the SHR group pericytes (*P* value < 0.05, Fold change > 1.5), of which 733 were upregulated and 623 downregulated. The genes with greatest betweenness centrality values were Itgb1, Vcam-1 and MMP-9. Based on KEGG analysis, 34 interacting signaling pathways and 43 interacting genes were screened, and MAPK, p53, Wnt, Jak-STAT, TGF-beta, VEGF and PPAR signaling pathways were the key nodes. Conclusions: Several DEGs and signaling pathways were identified in the brain microvascular pericytes of SHR rats compared to the WKY rats. Our findings will lay the foundation to study the role of brain microvascular pericytes in the development of spontaneous hypertension.

Keywords: Hypertension, RNA-Seq, differentially expressed genes, pathway analysis

Introduction

In recent years, with the change in people's diet and lifestyle, the number of patients with hypertension has increased all over the world. It is one of the main causes of death among cardiovascular and cerebrovascular diseases, due to the lack of clinical symptoms in the early stages, which hinders treatment and results in poor drug compliance in patients [1]. Vascular endothelial dysfunction [2, 3] and microcirculation [4, 5] are closely related with the pathogenesis of hypertension.

The endothelial injury induced by increased blood pressure reduces endothelium dependent vasodilatation and increases vasoconstriction, and blocks the interaction between endothelial and smooth muscle cells [6, 7]. In addition, the adhesion of inflammatory cells to the vascular walls and secretion of nitric oxide by intercellular adhesion molecules is increased in hypertensive patients [8, 9]. It enhances inflammatory response to the vascular walls, damages vascular endothelial cells and enhances platelet aggregation, eventually leading to atherosclerosis, thrombosis, organ damage, and further development of hypertension [10, 11]. In recent years, the role of microvessels in the development of cardiovascular disease has attracted a lot of attention. Microvessels are the sites of metabolite exchange, which is known as microcirculation. The changes in the structural domain of the small arter-

Table 1. RT-qPCR primers

Gene	Primer sequence (5'-3')	Gene	Primer sequence (5'-3')
FZD1	F: cacctggataggcatctggt	FGFR2	F: gttcaccctacccagggatt
	R: gtaacagccggacaggaaaa		R: gttcattggtgcagttggtg
SOD3	F: gacctggagatctggatgga	VEGFa	F: ttcctgcagcatagcagatg
	R: ggaccaagcctgtgatctgt		R: tttcttgcgctttcgttttt
Orm1	F: ttcagaccacagacgaccag	Lgfbp2	F: tgaaccccaatactgggaag
	R: ttttcactgctcctgcacac		R: atcattctcctgctgctcgt
Tsc22d3	F: ggtggccctagacaacaaga	Angptl2	F: ctgtgctcactccaacctca
	R: tcaaccagctcacgaatctg		R: ctcggaactcagcccagtag
Plac8	F: gcgatgaggactctctaccg	IL-33	F: tggcctcaccataagaaagg
	R: gatttggcacacagagcaaa		R: cctcccttcatgcttgctac
Lgfbp5	F: gaggctgtgaagaaggatcg	Adora2b	F: cctttggcattggactgact
	R: atctcaggtgcagggatgac		R: cagggcagcagctcttattc
Lgfbp3	F: ttccaagttccatccactcc	Adgrg1	F: gaagacttccgcttctgtgg
	R: ttctgggtgtctgtgctctg		R: gaggctctcgtctgtgttcc
MMP-9	F: cactgtaactgggggcaact	TIMP3	F: gctgtgcaactttgtggaga
	R: cacttcttgtcagcgtcgaa		R: ggtcacaaagcaaggcaagt
AQP1	F: ccgagacttaggtggctcag	Endod1	F: ccccttaacagtgacctcca
	R: ttgatcccacagccagtgta		R: gatcaaggctcggtccataa
THBS2	F: cagactggctatgcaggtga	FGFR3	F: atttagaccgcatcctcacg
	R: gtggcattggtagcacacac		R: caggtcatgggtgaacacag
EPHB2	F: gtacctggcggacatgaact	β-actin	F: cgttgacatccgtaaagacc
	R: gagagcccgaagtcagacac		R: ctaggagccagggcagtaatc

ies, arterioles and micro-vessels are important pathogenic bases for the organ damage seen in cardiovascular diseases [12]. Hypertension mainly causes a decrease in the diameter of the vessels and the small artery lumen, which leads to structural changes and vascular resistance [13]. It also decreases the density of blood vessels, including micro-vessels [14].

Pericytes, also known as Rouget cells, are contractile cells that wrap around the endothelial cells of capillaries throughout the body. They are embedded in the basement membrane of the endothelial cells, and communicate with them through direct physical contact and paracrine signals, to monitor and stabilize the maturation process of endothelial cells [15, 16]. Pericytes also regulate the microvessel blood flow [17], scavenge cell debris and control permeability of the blood brain barrier [16, 18]. However, no study so far has shown any association between cerebral microvascular pericytes and the pathogenesis of hypertension.

In this study, transcriptomes of pericytes from spontaneously hypertensive rats (SHR) and wild type Wistar Kyoto (WKY) rats were analyzed, and differentially expressed genes (DEGs) were screened, to determine their role in the pathogenesis of hypertension.

Materials and methods

Experimental animals

Animal experiments were approved by the Laboratory Animal Care and Ethics Committee of the Institute of Microcirculation, Chinese Academy of Medical Sciences & Peking Union Medical College. Thirteen-week-old male Wistar Kyoto (WKY) rats (n = 10) and spontaneously hypertensive rats (SHR) (n = 10) were purchased from Vital River Laboratory Animal Technology Co. Ltd. (license No. SCXK 2016-0006, Beijing, China).

Isolation of micro-vessels, culture and identification of pericytes

Immediately after decapitating the rats, their brains were ablated and immersed in ice-cold isolation buffer. Following tissue removal, micro-vessels were isolated as previously described [19, 20]. Briefly, the meninges and large pial vessels were carefully removed and regions of interest including the gray matter of the brain were isolated under a dissecting microscope. The brains were minced in ice-cold Dulbecco's modified Eagle's medium (DMEM), and digested in DMEM containing collagenase type II (1 mg/ml), DNase I (15 μg/ml) and gentamicin (50 μg/ml) for 1.5 h at 37°C. The digested micro-vessels were separated by centrifugation in 20% bovine serum albumin (BSA)/DMEM (1000 × g, 20 min). The pelleted micro-vessels were further digested with collagenase/dispase (1 mg/ml; Roche, Switherland) and DNaseI (6.7 μg/ml) in DMEM for 1 h at 37°C. The micro-vessel clusters were separated on a 33% continuous Percoll (GE Healthcare, UK) gradient (1000 × g, 10 min), and washed twice in DMEM. The resulting micro-

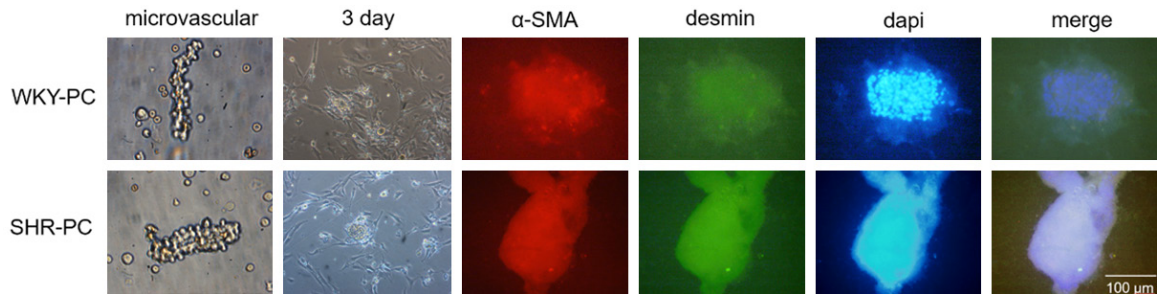

Figure 1. Isolation, cultivation and identification of pericytes from cerebral micro-vessels. The brain micro-vessels were isolated from the WKY and SHR rats and cultured in suitable medium. After 3 days, almost all of the pericytes had crawled out of the brain micro-vessels, and reached 80-90% confluency by the 7th day. They were double-labelled with PDGFRβ and NG2, and identified by fluorescence. Bar = 100 μm.

vessel fragments were seeded in an uncoated culture flask containing DMEM supplemented with 10% fetal bovine serum (FBS), 100 U/ml penicillin, and 100 μg/ml streptomycin. The culture medium was changed every 2 days. After 7 days of culture, after the pericytes had reached 80-90% confluence, the primary cultures were used for subsequent analyses. Immunocytochemistry was performed as previously described [21].

RNA extraction

Total RNA was extracted from the cells using the RNeasy Plus kit (Qiagen, USA), and dissolved in an appropriate amount of RNAase-free ddH_2O. The sample was further diluted 50 × in RNAase-free ddH_2O, and its concentration and purity were determined using NanoDrop 2000 (Thermo Scientific, USA). Furthermore, 1 μl RNA was taken from each sample and electrophoresed on a 1% agarose gel for 100 V × 30 min. The integrity of 18 s and 28 s rRNA bands were evaluated on a Bio-Rad gel imaging analyzer (Bio-Rad, USA).

Preparation of sequencing library and RNA-Seq

The cDNA library for RNA-Seq was constructed according to the instructions of the RNA-Seq Library Construction Kit (iCloning, USA) [22]. Briefly, oligo (dT) beads were used to enrich the mRNA and fragmented using the Fragmentation buffer. The first cDNA strand was synthesized using six-base random primers, followed by the addition of buffer solution, dNTPs, RNase H, and DNA polymerase I to synthesize the second cDNA strand. The cDNA was purified using the Qia Quick PCR Kit as per the manufacturer's instructions, and terminally ligated to poly (A) and sequencing adapters. A 200 bp fragment was selected by separation through 1.5% agarose gel electrophoresis. The cDNA library was then amplified by bridge PCR with the following conditions: initial denaturation at 98°C for 30 s, 15 cycles of 98°C 10 s, 65°C 30 s, 72°C 30 s, and final extension at 72°C for 5 min. The cDNA library was then sequenced using Illumina HiSeq 2000 high-throughput sequencer (Illumina, USA) using pair-end sequencing, with library size of 200 bp and read length of 116 nt [23].

Validation of RNA-Seq results

The RNA was reverse transcribed to cDNA by using PrimeScript™ RT reagent kit with gDNA Eraser kit (RR047A, Takara, Japan) with the following conditions: 37°C for 15 min and 85°C for 5 s. RT-qPCR reaction mix was prepared using 20 μl template and the SYBRTM Green PCR Master Mix (4312704, Invitrogen, German), and amplified in ABI 7300 Fluorescent Quantitative PCR instrument (Applied Biosystems, USA). The PCR parameters were: initial denaturation at 95°C for 30 sec, and 40 cycles of 90°C for 5 s and 65°C for 30 s. β-actin was used as the internal reference, and the relative expression of the target genes were calculated using the $2^{-\Delta t\Delta t}$ method. RT-qPCR primers were shown in **Table 1**.

Processing and assembly of sequencing raw data

The clean reads were obtained by removal of reads containing linkers, those with N greater than 5%, and whose base number with masses less than 20 were greater than 50%. The sequenced raw data processed by the HISAT2

Table 2. Representative display of DEGs

Ensembl Gene	Gene Name	*p*-value	q-value	Fold Change (SHR/WKY)	Syle
ENSRNOG00000016242	Fzd1	0.009329033	0.08659256	47.44948194	Up
ENSRNOG00000017206	Igfbp5	0.01313876	0.103819156	8.807374365	Up
ENSRNOG00000056135	Tsc22d3	0.000199895	0.022757597	12.11702988	Up
ENSRNOG00000003869	Sod3	0.001558853	0.045706919	45.05280292	Up
ENSRNOG00000007886	Orm1	1.89E-05	0.011879926	20.34257458	Up
ENSRNOG00000061910	Igfbp3	0.000141462	0.021436415	4.795145595	Up
ENSRNOG00000007886	Orm1	1.89E-05	0.011879926	20.34257458	Up
ENSRNOG00000002217	Plac8	0.000125619	0.02130323	9.230759055	Up
ENSRNOG00000017539	Mmp9	6.60E-06	0.008002092	7.265519367	Up
ENSRNOG00000011648	Aqp1	0.000649917	0.033239107	7.196132835	Up
ENSRNOG00000010529	Thbs2	0.000143189	0.021436415	2.097225521	Up
ENSRNOG00000012531	Ephb2	0.00159978	0.04647261	1.772122365	Up
ENSRNOG00000016374	Fgfr2	0.000834785	0.036132819	1.525621382	Up
ENSRNOG00000019598	Vegfa	0.009365149	0.086748099	1.782365629	Up
ENSRNOG00000016957	Igfbp2	8.44E-05	0.019068219	0.039638441	Down
ENSRNOG00000016678	Angptl2	0.000148746	0.021688543	0.099866321	Down
ENSRNOG00000002922	Adora2b	0.041773162	0.197873827	0.159245781	Down
ENSRNOG00000016456	IL-33	0.000114676	0.02130323	0.1922982	Down
ENSRNOG00000014963	Adgrg1	4.58E-05	0.01620986	0.213890382	Down
ENSRNOG00000004303	Timp3	0.001391624	0.043299044	0.654773419	Down
ENSRNOG00000024757	Endod1	0.00021152	0.022757597	0.076970779	Down
ENSRNOG00000016818	Fgfr3	0.006323075	0.079195013	0.503801675	Down

Ensembl Gene indicates the gene number in the Ensembl database; Gene Name indicates the gene name corresponding to the number; *p*-value indicates the significance level of the differential gene; Q-value indicates the misjudgment rate used to measure the reliability of the *p* value. Fold Change (SHR/WKY) indicates the ratio of the same gene signal value between the groups; Style indicates the up/down-regulation of genes according to the difference folds.

method were assembled into transcripts using the STINGTIE method of CTINGlinks software (University of California, Berkeley, USA) [24].

DEGs analysis

The RPKM (reads per kilo bases per million reads) method was used to calculate the expression of each gene and Ballgown method was used to compare the expression of the genes between different samples, and Student's t test was used to was used to compare differences between groups [25]. A DEG was defined as such when FDR ≤ 0.5 and differential expression ≥ 1.5. DAVID online analysis tool was used to perform functional cluster analysis of the DEGs [26] between the WKY and SHR groups, and their biological functions were determined according to the significant enrichment of GO terms. Fisher's exact test and multiple comparison test were used to calculate the significance level (*p*-value) and false positive rate (FDR) of each function, and the significant functions of the DEGs were screened with the threshold $p < 0.05$. Pathways that were significantly enriched among the DEGs were identified through KEGG analysis using Hypergeometric test. Pathways with FDR ≤ 0.5 were defined as significantly enriched.

Results

Morphology of pericytes from WKY and SHR and expression of generic markers

After 3 days of cultivation, almost all pericytes had crawled out of the brain micro-vessels, and 7 days later, reached 80-90% confluence. Co-expression of α-SMA and desmin, as determined by immuno-fluorescence, identified the isolated cells as pericytes (**Figure 1**).

Purity and integrity identification of total RNA

The OD260/OD280 ratios of total RNA extracted from 6 samples (WKY-PC1, WKY-PC2, WKY-PC3, SHR-PC1, SHR-PC2 and SHR-PC3) were greater than 1.8, indicating high purity RNA with no protein contamination. Good quality of

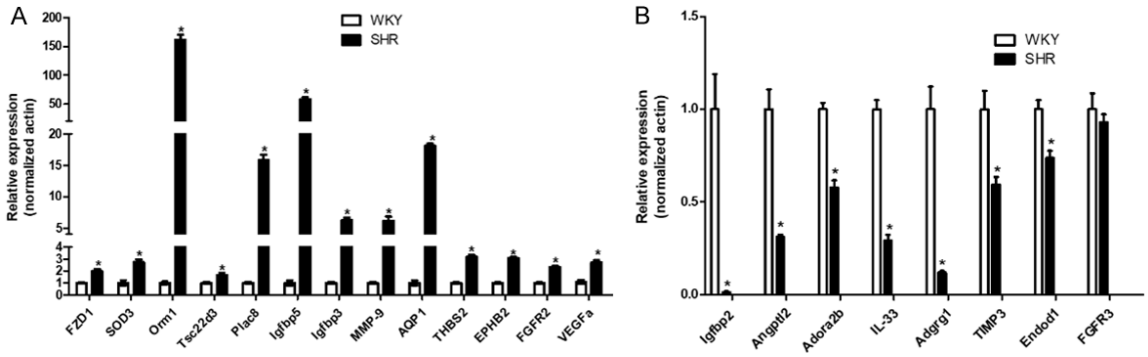

Figure 2. Partially differential gene expression obtained from RNA-Seq verified by RT-qPCR. Data are shown as mean ± SEM (Triple repeat), and Prism 5 statistical analysis software was used for statistical analysis of data, and Student's t test was used to was used to compare differences between groups. *indicates significant difference compared to WKY group, $P < 0.05$.

Table 3. Representative display of differential transcripts

Ensembl Transcript	Ensembl Gene	Gene Name	*p*-value	q-value	Fold Change (SHR/WKY)	Style
ENSRNOT00000089306	ENSRNOG00000038999	RT1-A1	0.001101339	0.054584506	354.7012198	Up
ENSRNOT00000050204	ENSRNOG00000031889	Rpl6-ps1	0.00000599	0.012240777	74.13574932	Up
ENSRNOT00000038660	ENSRNOG00000030712	RT1-A2	0.0000284	0.021118516	56.45090228	Up
ENSRNOT00000021979	ENSRNOG00000016242	Fzd1	0.012135564	0.119753845	50.90801758	Up
ENSRNOT00000005155	ENSRNOG00000003869	Sod3	0.001419572	0.05991521	46.70243702	Up
ENSRNOT00000080900	ENSRNOG00000038999	RT1-A1	0.0000788	0.027999441	42.90053763	Up
ENSRNOT00000022827	ENSRNOG00000016945	Pla2g2a	0.0000487	0.023695539	26.71388756	Up
ENSRNOT00000011327	ENSRNOG00000008465	Tmem176b	0.00336045	0.073992949	22.53151886	Up
ENSRNOT00000010454	ENSRNOG00000007886	Orm1	0.0000213	0.018620663	20.3252721	Up
ENSRNOT00000039551	ENSRNOG00000023383	Ddx3x	0.003758224	0.073992949	17.6106482	Up
ENSRNOT00000079919	ENSRNOG00000057626	Kif1b	0.005208051	0.073992949	0.105421906	Down
ENSRNOT00000022585	ENSRNOG00000016678	Angptl2	0.000157572	0.029371951	0.10011834	Down
ENSRNOT00000085692	ENSRNOG00000057823	Ubc	0.001145209	0.055281149	0.099517672	Down
ENSRNOT00000085516	ENSRNOG00000014630	Iws1	0.014457763	0.131881631	0.095341591	Down
ENSRNOT00000033969	ENSRNOG00000024757	Endod1	0.000246875	0.032140145	0.076939659	Down
ENSRNOT00000082645	ENSRNOG00000017191	Trim5	0.00019853	0.029399143	0.067549026	Down
ENSRNOT00000090051	ENSRNOG00000015320	Atp5g2	0.023390109	0.171763159	0.047122239	Down
ENSRNOT00000082538	ENSRNOG00000038999	RT1-A1	0.001067966	0.05399421	0.044663039	Down
ENSRNOT00000023068	ENSRNOG00000016957	Igfbp2	0.0000866	0.028016908	0.039305833	Down
ENSRNOT00000066363	ENSRNOG00000040287	Cyp1b1	0.005208051	0.073992949	0.017210797	Down

Ensembl Transcript indicates the number of transcripts in the Ensembl database; Ensembl Gene indicates the number of genes corresponding to the transcript in the Ensembl database; Gene Name indicates the gene name consistent with genetic identification of NCBI GenBank; *p*-value indicates the significance level of the differential gene; Q-value indicates the misjudgment rate used to measure the reliability of the *p* value. Fold-Change (SHR/WKY) indicates the fold difference, and the ratio of the detection value of the same transcript between groups; Style indicates transcript expression. The up/down-regulation of transcripts were determined according to the fold difference.

the isolated RNA was verified by 1% agarose gel electrophoresis in the form of intact 18 S and 28 S rRNA bands (Supplementary Figure 1).

Gene expression and transcript data analysis

A total of 1356 DEGs were observed between the pericytes of the experimental group (SHR) and the control group (WKY) with screening threshold of $P < 0.05$ and fold change greater than 1.5, of which 733 genes were upregulated and 623 were downregulated. To verify the accuracy of the sequencing results, 21 DEGs were amplified by real-time fluorescence quantitative PCR, and the results were consistent with the expression trends seen in RNA-Seq analysis (**Table 2**; **Figure 2**). Similarly, 1661 differential transcripts were obtained with *p*-value < 0.05 and fold change greater than 1.5, of which 893 had higher expression and 768 had

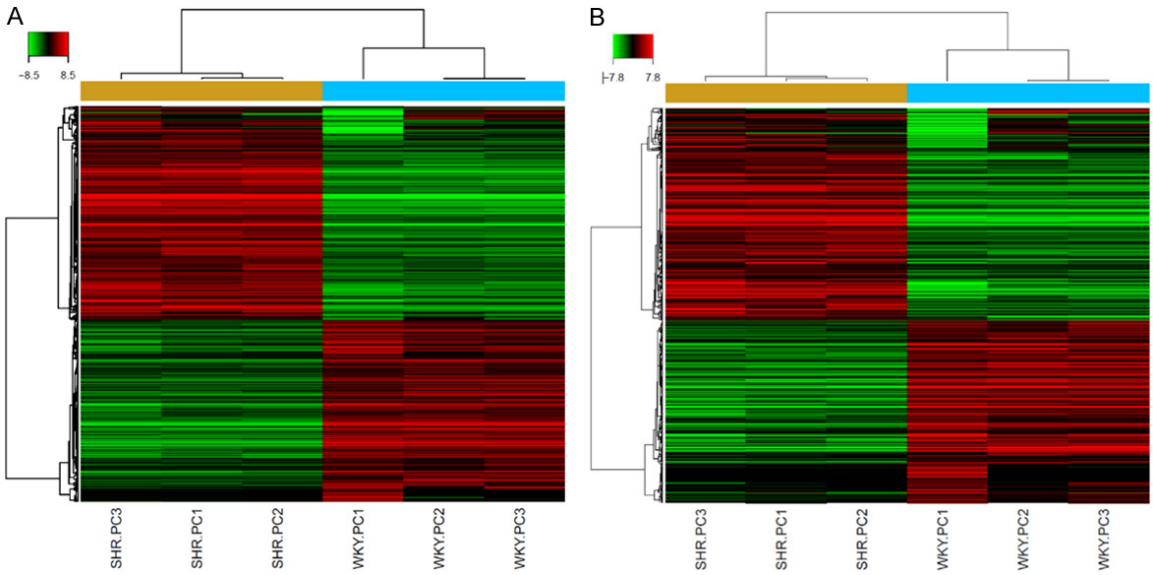

Figure 3. Dendrogram of (A) DEGs and (B). Transcripts. The abscissa represents the sample name, and the ordinate represents the differential genes. Red denotes upregulation, and green denotes downregulation of the DEGs.

Table 4. Representative display of GO function enrichment analysis of differential genes

Go-id	Go-name	Go-diffgene	Go-gene	Enrichment	*p*-value	FDR	Style
GO: 0008150	Biological_process	49	1408	2.309674827	3.26277E-07	4.09274E-05	Up
GO: 0043066	Negative regulation of Apoptotic process	35	478	4.859566881	9.19362E-14	3.07527E-11	Up
GO: 0051301	Cell division	31	152	13.53553798	2.39662E-25	4.81002E-22	Up
GO: 0055114	Oxidation-reduction process	27	210	8.533002743	9.36415E-17	4.69846E-14	Up
GO: 0045944	Positive regulation of transcription from RNA polymerase II promoter	27	715	2.50619661	6.31754E-05	0.003092511	Up
GO: 0008285	Negative regulation of cell proliferation	24	308	5.171516814	3.153E-10	7.91009E-08	Up
GO: 0042493	Response to drug	24	462	3.447677876	8.3662E-07	8.39548E-05	Up
GO: 0000122	Negative regulation of transcription from RNA polymerase II promoter	24	499	3.192038434	3.31446E-06	0.000289222	Up
GO: 0008284	Positive regulation of cell proliferation	23	388	3.934173659	1.41967E-07	1.98753E-05	Up
GO: 0006260	DNA replication	22	87	16.78266184	2.14613E-20	2.15365E-17	Up
GO: 0007067	Mitosis	22	111	13.1539782	6.40257E-18	4.28332E-15	Up
GO: 0008150	Biological_process	48	1408	2.759889435	1.41461E-09	6.83963E-07	Down
GO: 0042493	Response to drug	32	462	5.607394407	2.46757E-14	2.38614E-11	Down
GO: 0007155	Cell adhesion	31	260	9.652536383	1.22481E-20	2.36878E-17	Down
GO: 0045944	Positive regulation of transcription from RNA polymerase II promoter	25	715	2.830655831	1.66954E-05	0.000701933	Down
GO: 0045893	Positive regulation of transcription	23	495	3.761627082	3.25538E-07	3.49772E-05	Down
GO: 0007165	Signal transduction	22	377	4.724266973	1.09081E-08	2.63702E-06	Down
GO: 0006351	Transcription, DNA-dependent	21	640	2.656393581	0.000240624	0.006374892	Down
GO: 0008285	Negative regulation of cell proliferation	20	308	5.256932257	9.41845E-09	2.60218E-06	Down
GO: 0043065	Positive regulation of apoptotic process	19	258	5.961931699	2.95249E-09	1.14202E-06	Down
GO: 0008284	Positive regulation of cell Proliferation	19	388	3.964377264	1.97922E-06	0.000127594	Down

Go-id indicates the GO index number; Go-name indicates the GO name; Go-diffgene indicates the differential gene count enriched in a certain function; Go-gene represents the gene count or number of genes enriched a certain function; Enrichment represents the degree of enrichment; *p*-value was used to indicate the significance level of the difference genes; similar *p*-values indicates a greater degree of GO enrichment more likely to be affected by the experiment; FDR indicates the misjudgment rate of the *p*-value accuracy rate, and re-judgment of the GO significance level; Style indicates gene expression in and the up/down-regulation of transcripts were determined according to the fold difference.

lower expression in the pericytes of SHR group compared to the WKY group. The representative differential transcripts are shown in **Table 3**.

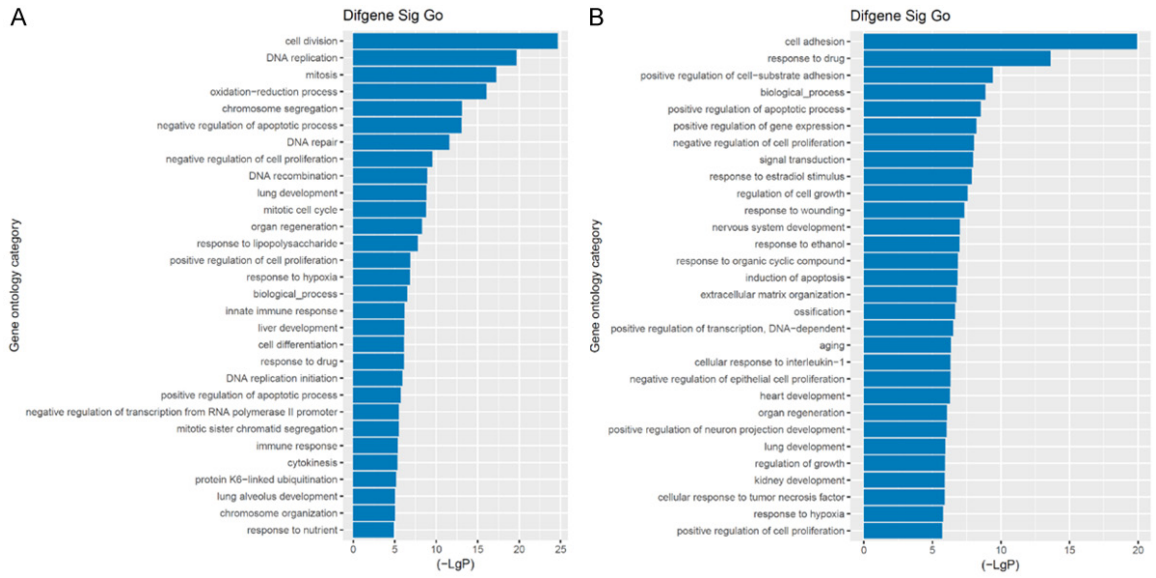

Figure 4. Functional enrichment of the DEGs (A). Up-regulated pathways in SHR compared to WKY; (B) Down-regulated pathways in SHR compared to WKY. The ordinate shows the name of the DEG function, and the abscissa indicates the negative logarithm of *p* value (-LgP). Higher -LgP corresponds to smaller *p* value and thus higher significance level of the DEG function.

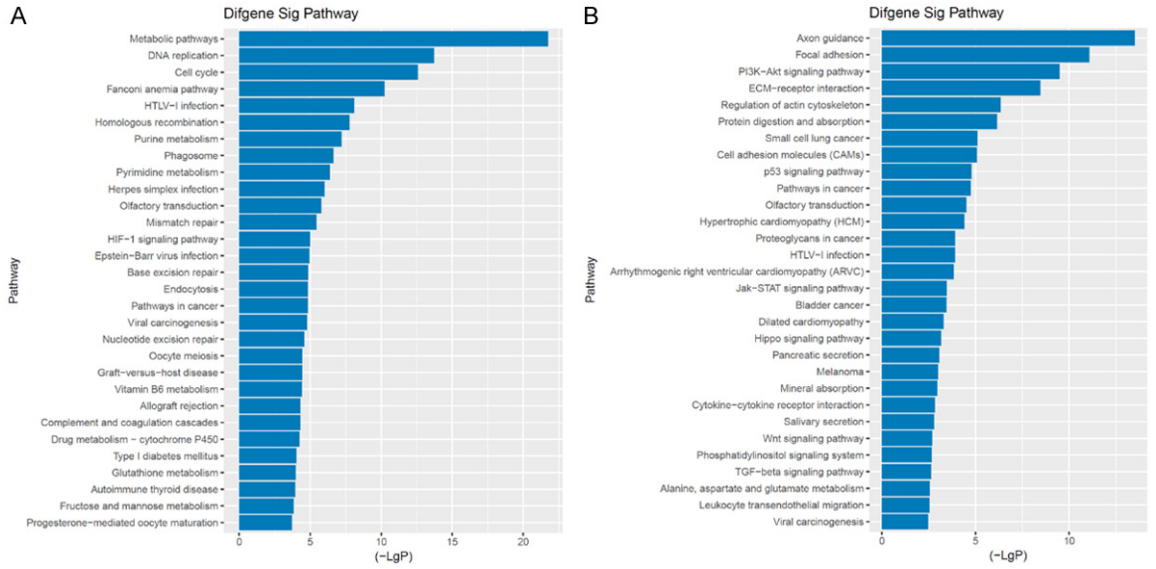

Figure 5. Histogram of significant pathways that are (A). Up-regulated and (B). Downregulated in SHR compared to WKY. The ordinate is the name of the DEG pathway, and the abscissa indicates the negative logarithm of *p* value (-LgP). Higher -LgP corresponds to smaller *p* value and thus higher significance level of the DEG pathway.

DEG cluster analysis and GO function enrichment analysis

The DEGs obtained by differential screening were clustered according to the signal values of each gene in the sample. Results showed intra-group and inter-group correlation, and similar expression of clustered genes indicated similar function (**Figure 3**).

GO analysis is used for functionally annotating genes based on the enrichment of certain terms in the Gene Ontology database, categorized under molecular functions (MF), cellular compartment (CC), and biological processes (BP). It helps discover the most important putative functions as well as non-functions of a large number of target genes [27, 28]. The top 10 most significantly up-regulated and

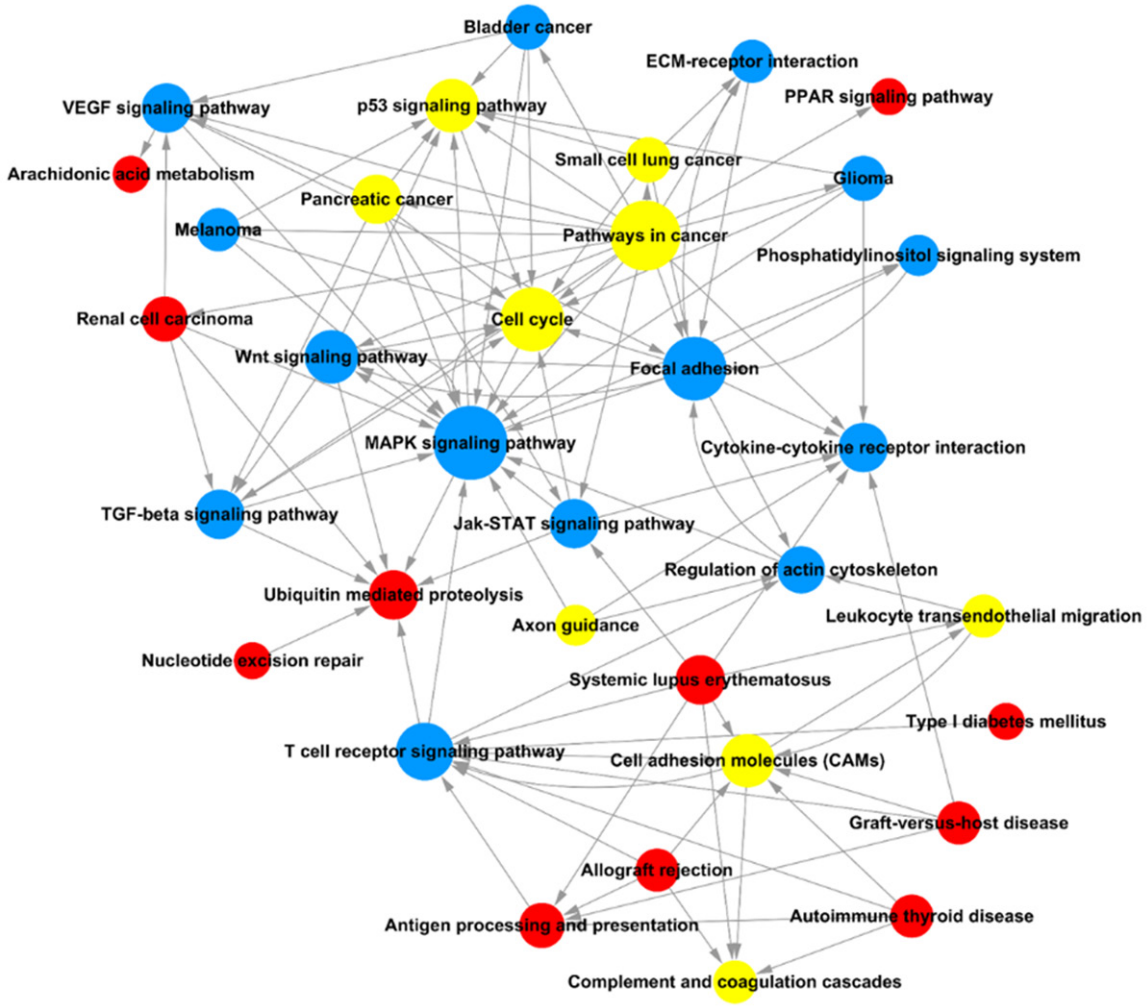

Figure 6. Interaction network of significant pathways. The circle represents the pathway and the line represents the relationship between the pathways. Red denotes pathways with up-regulated genes, blue denotes pathways with down-regulated genes, and yellow denotes pathways with both up-regulated and down-regulated genes.

10 down-regulated functions as per the GO-diffgene counts among the DEGs are shown in **Table 4**. The distribution map of the 30 most significant gene functions was constructed showing the up-regulation (**Figure 4A**) and down-regulation (**Figure 4B**) of gene functions.

Signaling pathway analysis of differential genes

KEGG (Kyoto Encyclopedia of Genes and Genomes) is a database that systematically analyzes the relationship between genes (and their encoded products) and their functions on a genome wide basis, as an entire network. KEGG pathway analysis was performed, and the threshold for the significant pathways involved with the DEGs was set using Fisher's exact test and Chi-square test, and p value < 0.05. The distribution map of the 30 most significant gene pathways was constructed for upregulated (**Figure 5A**) and downregulated pathways (**Figure 5B**).

Interaction network of significant pathways

The interaction network of the significant pathways obtained from KEGG analysis was constructed using Path-Net graph. From the network, signal-transduction relationship was systematically analyzed between sample significance pathway found by Pathway-Analysis, and it is possible to intuitively discover the important pathway's synergistic mode when sample changed and to systematically understand the nature of sample trait changes. Path-Net helps

Table 5. Interaction network node properties of significant pathways

Path-id	Path-name	Style	Indegree	Outdegree	Degree
Path: rno04010	MAPK signaling pathway	Down	15	4	19
Path: rno05200	Pathways in cancer	All	0	17	17
Path: rno04110	Cell cycle	All	12	2	14
Path: rno04510	Focal adhesion	Down	7	7	14
Path: rno04660	T cell receptor signaling pathway	Down	7	4	11
Path: rno04514	Cell adhesion molecules (CAMs)	All	6	3	9
Path: rno04115	p53 signaling pathway	All	8	1	9
Path: rno04310	Wnt signaling pathway	Down	3	6	9
Path: rno04060	Cytokine-cytokine receptor interaction	Down	7	0	7
Path: rno04630	Jak-STAT signaling pathway	Down	3	4	7
Path: rno05212	Pancreatic cancer	All	1	6	7
Path: rno05322	Systemic lupus erythematosus	Up	0	7	7
Path: rno04350	TGF-beta signaling pathway	Down	4	3	7
Path: rno04120	Ubiquitin mediated proteolysis	Up	7	0	7
Path: rno04370	VEGF signaling pathway	Down	4	3	7
Path: rno04810	Regulation of actin cytoskeleton	Down	4	2	6
Path: rno04612	Antigen processing and presentation	Up	4	1	5
Path: rno05219	Bladder cancer	Down	1	4	5
Path: rno05214	Glioma	Down	1	4	5
Path: rno05211	Renal cell carcinoma	Up	1	4	5
Path: rno05222	Small cell lung cancer	All	1	4	5
Path: rno05330	Allograft rejection	Up	0	4	4
Path: rno05320	Autoimmune thyroid disease	Up	0	4	4
Path: rno04610	Complement and coagulation cascades	All	4	0	4
Path: rno04512	ECM-receptor interaction	Down	3	1	4
Path: rno05332	Graft-versus-host disease	Up	0	4	4
Path: rno04670	Leukocyte transendothelial migration	All	2	2	4
Path: rno05218	Melanoma	Down	1	3	4
Path: rno04360	Axon guidance	All	0	3	3
Path: rno04070	Phosphatidylinositol signaling system	Down	2	1	3
Path: rno00590	Arachidonic acid metabolism	Up	1	0	1
Path: rno03420	Nucleotide excision repair	Up	0	1	1
Path: rno03320	PPAR signaling pathway	Up	1	0	1
Path: rno04940	Type I diabetes mellitus	Up	0	1	1

Path-id indicates the index number of pathway in the KEGG database; Path-name indicates the path name of the KEGG database; Style indicates the pathways with both up-regulated and down-regulated genes; Indegree indicates the number of upstream pathways; Outdegree indicates the number of downstream pathways; Degree indicates the number of upstream and downstream pathways.

find the most upstream and downstream signaling pathways in the network, and understand the relationship between these pathways. In this study, a total of 34 interacting signal pathways were screened, as shown in **Figure 6** and **Table 5**.

Intergenic interaction network

Based on the genes predicted with significant functions and the genes included in the significant pathways, a total of 333 GO-Pathway intersecting genes were obtained. By combining these intersecting genes and the KEGG database, the relationship between each gene with every other gene, as well as its upstream and downstream genes were determined. The inter-genic interaction was constructed as shown in **Figure 7** and **Table 6**. The genes Itgb1, Itgb3, Itgb4, Itgb6 and Itgb10 (with respective numbers 13, 10, 10, 10 and 10) were the most

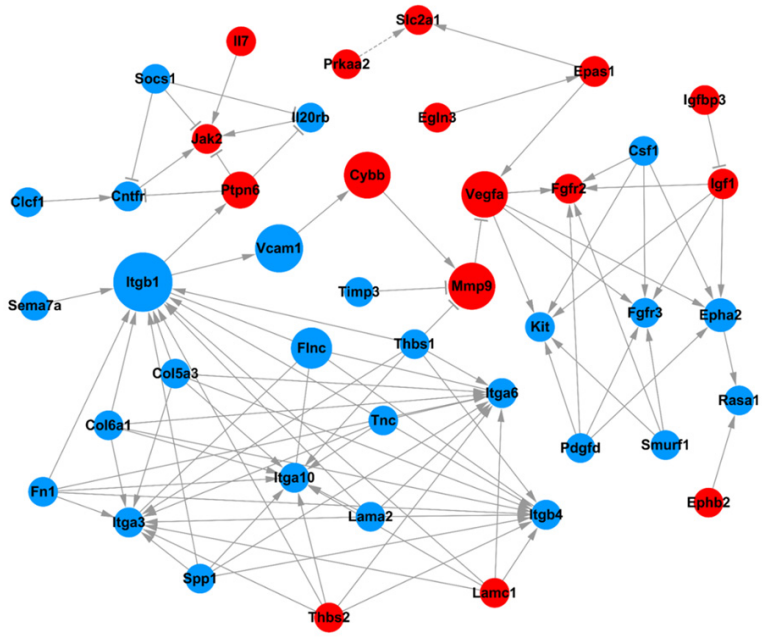

Figure 7. Intergenic interaction network. The circles represent the genes (red: up-regulated genes and blue: down-regulated genes). The size of the area represents the value of betweenness centrality, with greater values indicating higher signal transduction and regulation between two genes.

likely to interact with other genes, while Itgb1, Vcam1 and MMP9 had relatively stronger ability to regulate genes and were in key node positions throughout Signal-Net.

Discussions

Pericytes are contractile cells that are widely distributed throughout the microvascular walls, and together with endothelial cells regulate the blood flow [29, 30]. Recent studies have shown that pericytes not only maintain vascular structural integrity, but can also communicate with other endothelial cells through direct physical contact or paracrine signaling, and regulate blood perfusion in microcirculation, microvascular permeability, angiogenesis, wound healing, as well as maintain microvascular tone. Structural and functional abnormalities result in various microvascular diseases, such as diabetic retinopathy, coronary heart disease, hypertension, and tumor angiogenesis [31]. Recent studies on pericytes have elucidated their roles in various diseases, and their therapeutic potential has also attracted the attention of researchers [32, 33]. Pericytes differ across tissues on the basis of their anatomical locations around the micro-vessels, distribution density, phenotype, and differentiation characteristics. The density of microvascular pericytes is the highest in the central nervous system (CNS), where they play a crucial role in the formation and function of the blood-brain barrier [29]. One study found that the number of cerebral pericytes in spontaneously hypertensive rats were four times that of the healthy controls [34]. Our previous studies on pericytes were mainly focused on those of the CNS [21, 35], and therefore we selected brain microvascular pericytes for the present study as well.

The transcriptomes of brain microvascular pericytes isolated from normal (WKY) and hypertensive (SHR) rats were compared, and the DEGs were analyzed by bioinformatics. We obtained 1356 DEGs between the two groups (p value < 0.05, fold change > 1.5), and screened 34 interacting signaling pathways and 43 interacting genes on the basis of KEGG analysis. The significant pathways included the MAPK, p53, Wnt, Jak-STAT, TGF-beta, VEGF and PPAR signaling pathways, which have been implicated in the development of hypertension [36, 37]. Previous studies have shown that pericytes can also synthesize a variety of extracellular matrix (ECM) associated structures and adhesion proteins such as type I, type III, and type IV collagen, laminin and fibronectin [38], which are involved in the thickening of the microvascular basement membranes in patients with hypertension and diabetes mellitus (DM). In addition, the increase in myofilaments in the pericytes facilitates their migration and attachment. Previous studies had indicated that the change in the expression of adhesion and structural proteins in pericytes may be related to the occurrence and development of hypertension. The 34 interactive signaling pathways obtained in this study are also directly related to cell adhesion, including focal adhesion, cell adhesion molecules (CAMs), ECM-receptor interaction and regulation of actin cytoskeleton.

Table 6. Gene properties in gene interaction networks

Gene symbol	Description	Betweenness centrality	Degree	Indegree	Outdegree
Itgb1	Integrin subunit beta 1	0.045535297	13	11	3
Vcam1	Vascular cell adhesion molecule 1	0.028284245	2	1	1
Mmp9	Matrix metallopeptidase 9	0.026647966	4	3	1
Cybb	Cytochrome b-245 beta chain	0.026180458	2	1	1
Vegfa	Vascular endothelial growth factor A	0.02571295	6	2	4
Flnc	Filamin C	0.017765311	5	5	5
Ptpn6	Protein tyrosine phosphatase, non-receptor type 6	0.011220196	4	1	3
Epha2	Eph receptor A2	0.00631136	5	4	1
Epas1	Endothelial PAS domain protein 1	0.001636279	3	1	2
Igf1	Insulin-like growth factor 1	0.00116877	5	1	4
Itga10	Integrin subunit alpha 10	0.000420757	10	10	1
Itga3	Integrin subunit alpha 3	0.000420757	10	10	1
Itga6	Integrin subunit alpha 6	0.000420757	10	10	1
Itgb4	Integrin subunit beta 4	0.000420757	10	10	1
Cntfr	Ciliary neurotrophic factor receptor	0.000233754	4	3	1
Clcf1	Cardiotrophin-like cytokine factor 1	0	1	0	1
Col5a3	Collagen type V alpha 3 chain	0	5	0	5
Col6a1	Collagen type VI alpha 1 chain	0	5	0	5
Csf1	Colony stimulating factor 1	0	4	0	4
Egln3	Egl-9 family hypoxia-inducible factor 3	0	1	0	1
Ephb2	Eph receptor B2	0	1	0	1
Fgfr2	Fibroblast growth factor receptor 2	0	5	5	0
Fgfr3	Fibroblast growth factor receptor 3	0	5	5	0
Fn1	Fibronectin 1	0	5	0	5
Igfbp3	Insulin-like growth factor binding protein 3	0	1	0	1
Il20rb	Interleukin 20 receptor subunit beta	0	3	2	1
Il7	Interleukin 7	0	1	0	1
Jak2	Janus kinase 2	0	5	5	0
Kit	KIT proto-oncogene receptor tyrosine kinase	0	5	5	0
Lama2	Laminin subunit alpha 2	0	5	0	5
Lamc1	Laminin subunit gamma 1	0	5	0	5
Pdgfd	Platelet derived growth factor D	0	4	0	4
Prkaa2	Protein kinase AMP-activated catalytic subunit alpha 2	0	1	0	1
Rasa1	RAS p21 protein activator 1	0	2	2	0
Sema7a	Semaphorin 7A (John Milton Hagen blood group)	0	1	0	1
Slc2a1	Solute carrier family 2 member 1	0	2	2	0
Smurf1	SMAD specific E3 ubiquitin protein ligase 1	0	3	0	3
Socs1	Suppressor of cytokine signaling 1	0	3	0	3
Spp1	Secreted phosphoprotein 1	0	5	0	5
Thbs1	Thrombospondin 1	0	6	0	6
Thbs2	Thrombospondin 2	0	5	0	5
Timp3	TIMP metallopeptidase inhibitor 3	0	1	0	1
Tnc	Tenascin C	0	5	0	5

Gene symbol is the name of the gene identified in NCBI database; Description is the annotation of the gene; Betweenness centrality indicates the center of signal transduction, with higher values corresponding to stronger signal transduction; Indegree indicates the number of upstream genes; Outdegree indicates the number of downstream genes; Degree indicates the number of upstream and downstream genes of a certain gene.

Ubiquitination is an important post-translational modification that regulates biological processes such as cell proliferation, differentiation, and apoptosis. Dysregulated ubiquitina-

tion causes abnormal functional changes in proteins, which are related to various diseases. Disrupted ubiquitination is associated with Liddle syndrome, an autosomal dominant disorder characterized by salt-sensitive hypertension and hypokalemic alkalosis. A mutation in the renal epithelial sodium channel gene results in its abnormal degradation by the ubiquitinin proteasome system, resulting in the clinical features of the disease. Several subsequent studies have also reported a role of ubiquitination in the occurrence and development of salt-sensitive hypertension and blood pressure regulation [39, 40]. In this study also, the ubiquitin mediated proteolysis signaling pathway was significantly altered in the cerebral microvascular pericytes of spontaneously hypertensive rats. The metabolites of arachidonic acid, an essential fatty acid, have important regulatory roles in many physiological and pathological processes. Arachidonic acid is metabolized through three major pathways involving cyclooxygenase, lipoxygenase and cytochrome P450. Studies have shown [41, 42] that cytochrome 450, the key gene in the cytochrome P450 metabolic pathway affects hypertension by regulating the downstream metabolites such as 20-hydroxyeicosatetraenoic acid of w-hydroxylase and epoxygenase [43, 44].

We also explored the relationship between the target genes by constructing a network of the DEGs, and identifying the upstream and downstream proteins of these genes. 'Betweenness centrality' represents the mediating ability of each gene in an interaction network; greater the Betweenness centrality, greater is the extent of signaling between the genes. The 3 genes with the highest values were Itgb1 (integrin subunit beta 1), Vcam-1 and MMP-9. Integrin is a transmembrane receptor that mediates the communication between cells and with their external environment via the beta 1 subunit, and transmits the changes in the chemical and mechanical characteristics of ECM to the cells. During normal blood flow, Itgb1 expression is uniform along the capillary loop, while in abnormal hemodynamic conditions such as acute hypertension, the expression of Itgb1 is reduced. However, the specific mechanism of Itgb1 regulation in abnormal blood flow is not clear [45, 46].

Vcam-1 is an important cell adhesion molecule, which is induced by inflammatory cytokines [47], and is an important marker for activated vascular endothelial cells. The activation of endothelial cells can directly cause cell injury and vascular inflammation, which are important steps in the pathogenesis of hypertension [48, 49]. Vcam-1 not only plays an important role in immunological and inflammatory responses, but also promotes the synthesis and secretion of various vasoactive substances [50, 51]. MMP-9, one of the most important members of the MMPs family, is produced by the smooth muscle cells following stimulation by the vascular endothelium during chronic hypertension. It degrades the extracellular matrix of blood vessels to destroy vascular walls, and causes vascular remodeling [52, 53]. The latter is a dynamic process including cell proliferation, migration, apoptosis, and matrix synthesis, degradation and rearrangement. It is an important pathological basis for the initiation and progression of hypertension. Therefore, MMP-9 triggers hypertension by inducing vascular remodeling.

Conclusions

Spontaneous hypertension induces changes in gene expression in rat brain microvascular pericytes. The DEGs in cerebral microvascular pericytes of the hypertensive rats were enriched in the GO terms of molecular functions, celluler compartment and biological processes. Our study lays the foundation for understanding the gene expression changes in pericytes, which play an important role in microcirculation, and our future efforts will be focused on elucidating the mechanism of pericytes and endothelial cells interaction.

Acknowledgements

This study was supported by CAMS Initiative for Innovative Medicine (CAMS-I2M) (2016-I2M-3-006) and the innovation fund of Chinese Academy of Medical Sciences and Peking Union Medical College (3332015123).

Disclosure of conflict of interest

None.

Address correspondence to: Drs. Qingbin Wu and Honggang Zhang, Institute of Microcirculation, Chinese Academy Medical Sciences & Pecking Union Medical College, 5, Dong Dan San Tiao, Beijing 100005, China. Tel: 0086-10-65126407; Fax: 0086-10-65251957; E-mail: wuqingbin@imc.pumc.edu.cn (QBW); zhanghg1966126@163.com (HGZ)

References

[1] Messerli FH, Fischer U, Rimoldi SF and Bangalore S. Hypertension control and cardiovascular disease. Lancet 2017; 389: 153.

[2] Jurva JW, Phillips SA, Syed AQ, Syed AY, Pitt S, Weaver A and Gutterman DD. The effect of exertional hypertension evoked by weight lifting on vascular endothelial function. J Am Coll Cardiol 2006; 48: 588-589.

[3] Wong WT, Wong SL, Tian XY and Huang Y. Endothelial dysfunction: the common consequence in diabetes and hypertension. J Cardiovasc Pharm 2010; 55: 300-307.

[4] Pries AR. Perspectives: microcirculation in hypertension and cardiovascular disease. Eur Heart J Suppl 2014; 16: A28-A29.

[5] Strain WD, Adingupu DD and Shore AC. Microcirculation on a large scale: techniques, tactics and relevance of studying the microcirculation in larger population samples. Microcirculation 2012; 19: 37-46.

[6] Puddu P, Puddu GM, Zaca F and Muscari A. Endothelial dysfunction in hypertension. Acta Cardiol 2000; 55: 3-12.

[7] Rekhviashvili A and Abashidze R. The relationship between endothelial dysfunction and 24-hour blood pressure rhythm in patients with arterial hypertension. Georgian Med News 2008; 25: 13-7.

[8] Schulz E, Jansen T, Wenzel P, Daiber A and Münzel T. Nitric oxide, tetrahydrobiopterin, oxidative stress, and endothelial dysfunction in hypertension. Antioxid Redox Sign 2008; 10: 1115-26.

[9] Klinger JR, Abman SH and Gladwin MT. Nitric oxide deficiency and endothelial dysfunction in pulmonary arterial hypertension. Am J Resp Crit Car 2013; 188: 639-646.

[10] Gamboa A, Figueroa R, Paranjape SY, Farley G, Diedrich A and Biaggioni I. Autonomic blockade reverses endothelial dysfunction in obesity-associated hypertension. Hypertension 2016; 68: 1004-10.

[11] Virdis A and Taddei S. Endothelial dysfunction in resistance arteries of hypertensive humans: old and new conspirators. J Cardiovasc Pharm 2016; 67: 451-7.

[12] Rusavy Z, Pitrova B, Korecko V, Kalis V. Changes in capillary diameters in pregnancy-induced hypertension. Hypertens Pregncy 2015; 34: 307-13.

[13] Mulvany MJ. Small artery structure: time to take note? Am J Hypertens 2007; 20: 853-854.

[14] Renna NF, Heras NDL and Miatello RM. Pathophysiology of vascular remodeling in hypertension. Int J Hyperten 2013; 2013: 808353.

[15] Greenberg JI, Shields DJ, Barillas SG, Acevedo LM, Murphy E, Huang J, Scheppke L, Stockmann C, Johnson RS and Angle N. A role for VEGF as a negative regulator of pericyte function and vessel maturation. Nature 2008; 456: 809-13.

[16] Stapor PC, Sweat RS, Dashti DC, Betancourt AM and Murfee WL. Pericyte dynamics during angiogenesis: new insights from new identities. J Vasc Res 2014; 51: 163-74.

[17] Yemisci M, Gursoyozdemir Y, Vural A, Can A, Topalkara K and Dalkara T. Pericyte contraction induced by oxidative-nitrative stress impairs capillary reflow despite successful opening of an occluded cerebral artery. Nat Med 2009; 15: 1031-1037.

[18] Sims DE. Recent advances in pericyte biology-implications for health and disease. Can J Cardiol 1991; 7: 431-443.

[19] Dohgu S, Takata F, Yamauchi A, Nakagawa S, Egawa T, Naito M, Tsuruo T, Sawada Y, Niwa M and Kataoka Y. Brain pericytes contribute to the induction and up-regulation of blood-brain barrier functions through transforming growth factor-beta production. Brain Res 2005; 1038: 208-215.

[20] Nakagawa S, Deli MA, Nakao S, Honda M, Hayashi K, Nakaoke R, Kataoka Y and Niwa M. Pericytes from brain microvessels strengthen the barrier integrity in primary cultures of rat brain endothelial cells. Cell Mol Neurobiol 2007; 27: 687-694.

[21] Wu Q, Jing Y, Yuan X, Li B, Wang B, Liu M, Li H and Xiu R. The distinct abilities of tube-formation and migration between brain and spinal cord microvascular pericytes in rats. Clin Hemorheol Micro 2015; 60: 231-240.

[22] Tariq MA, Kim HJ, Jejelowo O and Pourmand N. Whole-transcriptome RNAseq analysis from minute amount of total RNA. Nucleic Acids Res 2011; 39: e120.

[23] Croucher NJ, Fookes MC, Perkins TT, Turner DJ, Marguerat SB, Keane T, Quail MA, He M, Assefa S, Bähler J, Kingsley RA, Parkhill J, Bentley SD, Dougan G and Thomson NR. A simple method for directional transcriptome sequencing using Illumina technology. Nucleic Acids Res 2009; 37: e148.

[24] Trapnell C, Roberts A, Goff L, Pertea G, Kim D, Kelley DR, Pimentel H, Salzberg SL, Rinn JL and Pachter L. Differential gene and transcript expression analysis of RNA-seq experiments with TopHat and Cufflinks. Nat Protoc 2012; 7: 562-78.

[25] Mortazavi A, Williams BA, McCue K, Schaeffer L and Wold B. Mapping and quantifying mammalian transcriptomes by RNA-Seq. Nat Methods 2008; 5: 621-8.

[26] Huang da W, Sherman BT and Lempicki RA. Systematic and integrative analysis of large gene lists using DAVID bioinformatics resources. Nat Protoc 2008; 4: 44-57.
[27] Young MD, Wakefield MJ, Smyth GK and Oshlack A. Gene ontology analysis for RNA-seq: accounting for selection bias. Genome Biol 2010; 11: R14.
[28] Ashburner M, Ball CA, Blake JA, Botstein D, Butler H, Cherry JM, Davis AP, Dolinski K, Dwight SS and Eppig JT. Gene ontology: tool for the unification of biology. Nat Genet 2000; 25: 25-9.
[29] Vezzani B, Pierantozzi E and Sorrentino V. Not all pericytes are born equal: pericytes from human adult tissues present different differentiation properties. Stem Cells Dev 2016; 25: 1549-1558.
[30] Bergers G and Song S. The role of pericytes in blood-vessel formation and maintenance. Neuro Oncol 2005; 7: 452-464.
[31] Birbrair A, Zhang T, Wang Z-M, Messi ML, Mintz A and Delbono O. Pericytes at the intersection between tissue regeneration and pathology. Clin Sci 2015; 128: 81-93.
[32] O'farrell FM and Attwell D. A role for pericytes in coronary no-reflow. Nat Rev Cardiol 2014; 11: 427-32.
[33] Murray IR, Baily JE, Chen WC, Dar A, Gonzalez ZN, Jensen AR, Petrigliano FA, Deb A and Henderson NC. Skeletal and cardiac muscle pericytes: functions and therapeutic potential. Pharmacol Therapeut 2017; 171: 65-74.
[34] Allt G and Lawrenson J. Pericytes: cell biology and pathology. Cells Tissues Organs 2001; 169: 1-11.
[35] Wu Q, Jing Y, Yuan X, Zhang X, Li B, Liu M, Wang B, Li H, Liu S and Xiu R. Melatonin treatment protects against acute spinal cord injury-induced disruption of blood spinal cord barrier in mice. J Mol Neurosci 2014; 54: 714-722.
[36] Dasinger JH, Davis GK, Newsome AD and Alexander BT. The developmental programming of hypertension: physiological mechanisms. Hypertension 2016; 68: 826-31.
[37] Johns DG, Dorrance AM, Leite R, Weber DS and Webb RC. Novel signaling pathways contributing to vascular changes in hypertension. J Biomed Sci 2000; 7: 431-443.
[38] Kim JA, Tran ND, Li Z, Yang F, Zhou W and Fisher MJ. Brain endothelial hemostasis regulation by pericytes. J Cerebr Blood F Met 2006; 26: 209-217.
[39] Boyden LM, Choi M, Choate KA, Nelson-Williams CJ, Farhi A, Toka HR, Tikhonova IR, Bjornson R, Mane SM, Colussi G, Lebel M, Gordon RD, Semmekrot BA, Poujol A, Välimäki MJ, De Ferrari ME, Sanjad SA, Gutkin M, Karet FE, Tucci JR, Stockigt JR, Keppler-Noreuil KM, Porter CC, Anand SK, Whiteford ML, Davis ID, Dewar SB, Bettinelli A, Fadrowski JJ, Belsha CW, Hunley TE, Nelson RD, Trachtman H, Cole TR, Pinsk M, Bockenhauer D, Shenoy M, Vaidyanathan P, Foreman JW, Rasoulpour M, Thameem F, Al-Shahrouri HZ, Radhakrishnan J, Gharavi AG, Goilav B, Lifton RP. Mutations in kelch-like 3 and cullin 3 cause hypertension and electrolyte abnormalities. Nature 2012; 482: 98-102.
[40] Ronzaud C, Loffing-Cueni D, Hausel P, Debonneville A, Malsure SR, Fowler-Jaeger N, Boase NA, Perrier R, Maillard M and Yang B. Renal tubular NEDD4-2 deficiency causes NCC-mediated salt-dependent hypertension. J Clin Invest 2013; 123: 657-665.
[41] Savas Ü, Wei S, Hsu MH, Falck JR, Guengerich FP, Capdevila JH and Johnson EF. 20-Hydroxyeicosatetraenoic Acid (HETE) dependent hypertension in human cytochrome P450 (CYP) 4A11 transgenic mice: normalization of blood pressure by sodium restriction, hydrochlorothiazide, or blockade of the type 1 angiotensin II receptor. J Biol Chem 2016; 291: 16904-16919.
[42] Makita K, Takahashi K, Karara A, Jacobson HR, Falck JR and Capdevila JH. Experimental and/or genetically controlled alterations of the renal microsomal cytochrome P450 epoxygenase induce hypertension in rats fed a high salt diet. J Clin Invest 1994; 94: 2414-2420.
[43] Spector AA. Arachidonic acid cytochrome P450 epoxygenase pathway. J Lipid Res 2009; 50: S52-S56.
[44] Sarkis A and Roman R. Role of cytochrome P450 metabolites of arachidonic acid in hypertension. Curr Drug Metab 2004; 5: 245-256.
[45] Essex R. Using microfluidic models to determine the effects of cd151 and the integrin subunit & beta1 on tumor cell adhesion. J Environ Manage 2008; 86: 282.
[46] Lee K, Boctor S, Barisoni LM and Gusella GL. Inactivation of integrin-beta1 prevents the development of polycystic kidney disease after the loss of polycystin-1. J Am Soc Nephrol 2015; 26: 888-895.
[47] Fang L, Yan Y, Komuves LG, Yonkovich S, Sullivan CM, Stringer B, Galbraith S, Lokker NA, Hwang SS and Nurden P. PDGF C is a selective alpha platelet-derived growth factor receptor agonist that is highly expressed in platelet alpha granules and vascular smooth muscle. Arterioscler Thromb Vasc Biol 2004; 24: 787-92.
[48] Gupta V, Sachdeva S, Khan AS and Haque SF. Endothelial dysfunction and inflammation in different stages of essential hypertension. Saudi J Kidney Dis Transpl 2011; 22: 97-103.
[49] Androulakis ES, Tousoulis D, Papageorgiou N, Tsioufis C, Kallikazaros I and Stefanadis C. Essential hypertension: is there a role for in-

flammatory mechanisms? Cardiol Rev 2015; 17: 216-21.
[50] Linhartova K, Sterbakova G, Racek J, Cerbak R, Porazikova K and Rokyta R. Linking soluble vascular adhesion molecule-1 level to calcific aortic stenosis in patients with coronary artery disease. Exp Clin Cardiol 2009; 14: 80-83.
[51] Desouza CA, Dengel DR, Macko RF, Cox K and Seals DR. Elevated levels of circulating cell adhesion molecules in uncomplicated essential hypertension. Am J Hypertens 1997; 10: 1335-41.
[52] Flamant M, Placier S, Dubroca C, Esposito B, Lopes I, Chatziantoniou C, Tedgui A, Dussaule JC and Lehoux S. MMP9 induces vascular remodeling and curbs early hypertension in angiotensin II-infused mice. J Vasc Res 2005; 42: 75-75.
[53] Deng J, Zhang J, Feng C, Xiong L and Zuo Z. Critical role of matrix metalloprotease-9 in chronic high fat diet-induced cerebral vascular remodelling and increase of ischaemic brain injury in mice. Cardiovasc Res 2014; 103: 473-484.

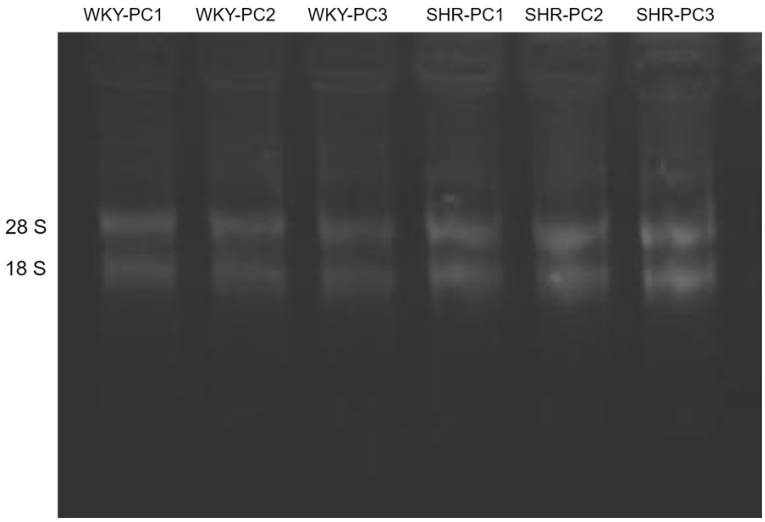

Supplementary Figure 1. Integrity of total RNA sample detected by 1% agarose gel electrophoresis.